

# Distributed-Memory Randomized Algorithms for Sparse Tensor CP Decomposition

Vivek Bharadwaj  
University of California, Berkeley  
Berkeley, CA, USA  
vivek\_bharadwaj@berkeley.edu

Osman Asif Malik\*  
Encube Technologies  
Stockholm, Sweden  
osman@getencube.com

Riley Murray†  
Sandia National Laboratories  
Albuquerque, NM, USA  
rjmurr@sandia.gov

Aydın Buluç  
Lawrence Berkeley National  
Laboratory  
Berkeley, CA, USA  
abuluc@lbl.gov

James Demmel  
University of California, Berkeley  
Berkeley, CA, USA  
demmel@berkeley.edu

## ABSTRACT

Candecomp / PARAFAC (CP) decomposition, a generalization of the matrix singular value decomposition to higher-dimensional tensors, is a popular tool for analyzing multidimensional sparse data. On tensors with billions of nonzero entries, computing a CP decomposition is a computationally intensive task. We propose the first distributed-memory implementations of two randomized CP decomposition algorithms, CP-ARLS-LEV and STS-CP, that offer nearly an order-of-magnitude speedup at high decomposition ranks over well-tuned non-randomized decomposition packages. Both algorithms rely on leverage score sampling and enjoy strong theoretical guarantees, each with varying time and accuracy tradeoffs. We tailor the communication schedule for our random sampling algorithms, eliminating expensive reduction collectives and forcing communication costs to scale with the random sample count. Finally, we optimize the local storage format for our methods, switching between analogues of compressed sparse column and compressed sparse row formats. Experiments show that our methods are fast and scalable, producing 11x speedup over SPLATT by decomposing the billion-scale Reddit tensor on 512 CPU cores in under two minutes.

## CCS CONCEPTS

• **Theory of computation** → **Massively parallel algorithms; Random projections and metric embeddings.**

## KEYWORDS

Sparse Tensors, CP Decomposition, Randomized Linear Algebra, Leverage Score Sampling

\*Work completed while author was affiliated with Lawrence Berkeley National Laboratory.

†Work completed while author was affiliated with Lawrence Berkeley National Laboratory, International Computer Science Institute, and University of California, Berkeley.

Permission to make digital or hard copies of part or all of this work for personal or classroom use is granted without fee provided that copies are not made or distributed for profit or commercial advantage and that copies bear this notice and the full citation on the first page. Copyrights for third-party components of this work must be honored. For all other uses, contact the owner/author(s).

SPAA '24, June 17–21, 2024, Nantes, France

© 2024 Copyright held by the owner/author(s).

ACM ISBN 979-8-4007-0416-1/24/06.

<https://doi.org/10.1145/3626183.3659980>

## ACM Reference Format:

Vivek Bharadwaj, Osman Asif Malik, Riley Murray, Aydın Buluç, and James Demmel. 2024. Distributed-Memory Randomized Algorithms for Sparse Tensor CP Decomposition. In *Proceedings of the 36th ACM Symposium on Parallelism in Algorithms and Architectures (SPAA '24), June 17–21, 2024, Nantes, France*. ACM, New York, NY, USA, 14 pages. <https://doi.org/10.1145/3626183.3659980>

## 1 INTRODUCTION

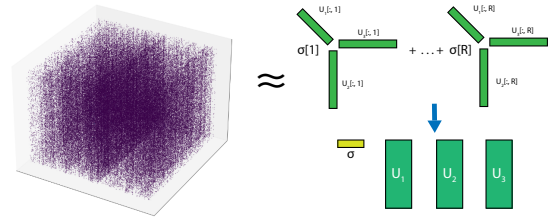


**Figure 1: A subset of entries from the 3D Amazon Review sparse tensor [1] and its illustrated CP decomposition. The sparse tensor is approximated by a sum of 3D outer products of vectors, which are columns of factor matrices  $U_1$ ,  $U_2$ , and  $U_3$ . Outer products are scaled by elements of  $\sigma$ .**

Randomized algorithms for numerical linear algebra have become increasingly popular in the past decade, but their distributed-memory communication characteristics and scaling properties have received less attention. In this work, we examine randomized algorithms to compute the Candecomp / PARAFAC (CP) decomposition, a generalization of the matrix singular-value decomposition to a number of modes  $N > 2$ . Given a tensor  $\mathcal{T} \in \mathbb{R}^{I_1 \times \dots \times I_N}$  and a target rank  $R$ , the goal of CP decomposition (illustrated in Figure 1) is to find a set of *factor matrices*  $U_1, \dots, U_N, U_j \in \mathbb{R}^{I_j \times R}$  with unit norm columns and a nonnegative vector  $\sigma \in \mathbb{R}^R$  satisfying

$$\mathcal{T}[i_1, \dots, i_N] \approx \sum_{r=1}^R \sigma[r] * U_1[i_1, r] * \dots * U_N[i_N, r]. \quad (1)$$

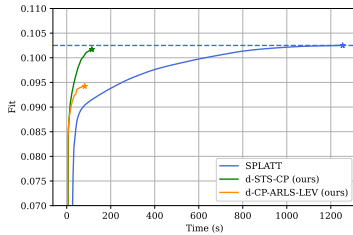


**Figure 2: Running maximum accuracy over time for SPLATT, a state-of-the-art distributed CP decomposition software package, and our randomized algorithms on the Reddit tensor, target rank  $R = 100$ , on 512 CPU cores. Curves are averages of 5 trials, 80 ALS rounds.**

We consider real **sparse** tensors  $\mathcal{T}$  with  $N \geq 3$ , all entries known, and billions of nonzero entries. Sparse tensors are a flexible abstraction for a variety of data, such as network traffic logs [2], text corpora [1], and knowledge graphs [3].

## 1.1 Motivation

Why is a low-rank approximation of a sparse tensor useful? We can view the sparse CP decomposition as an extension of well-studied sparse matrix factorization methods, which can mine patterns from large datasets [4]. Each row of the CP factors is a dense embedding vector for an index  $i_j \in [I_j]$ ,  $1 \leq j \leq N$ . Because each embedding is a small dense vector while the input tensor is sparse, sparse tensor CP decomposition may incur high relative error with respect to the input and rarely captures the tensor sparsity structure exactly. Nevertheless, the learned embeddings contain valuable information. CP factor matrices have been successfully used to identify patterns in social networks [5, 6], detect anomalies in packet traces [2], and monitor trends in internal network traffic [7]. As we discuss below, a wealth of software packages exist to meet the demand for sparse tensor decomposition.

One of the most popular methods for computing a sparse CP decomposition, the *Alternating-Least-Squares* (ALS) algorithm, involves repeatedly solving large, overdetermined linear least-squares problems with structured design matrices [8]. High-performance libraries DFacto[9], SPLATT [10], HyperTensor [11], and BigTensor [12] distribute these expensive computations to a cluster of processors that communicate through an interconnect. Separately, several works use randomized sampling methods to accelerate the least-squares solves, with prototypes implemented in a shared-memory setting [6, 13–15]. These randomized algorithms have strong theoretical guarantees and offer significant asymptotic advantages over non-randomized ALS. Unfortunately, prototypes of these methods require hours to run [6, 15] and are neither competitive nor scalable compared to existing libraries with distributed-memory parallelism.

## 1.2 Our Contributions

We propose the first distributed-memory parallel formulations of two randomized algorithms, CP-ARLS-LEV [6] and STS-CP [15], with accuracy identical to their shared-memory prototypes. We

then provide implementations of these methods that scale to thousands of CPU cores. We face **dual technical challenges** to parallel scaling. First, sparse tensor decomposition generally has lower arithmetic intensity (FLOPs / data word communicated between processors) than dense tensor decomposition, since computation scales linearly with the tensor nonzero count. Some sparse tensors exhibit nonzero fractions as low as  $4 \times 10^{-10}$  (see Table 4), while the worst-case communication costs for sparse CP decomposition remain identical to the dense tensor case [16]. Second, randomized algorithms can save an order of magnitude in computation over their non-randomized counterparts [17–19], but their inter-processor communication costs remain unaltered unless carefully optimized. Despite these compounding factors that reduce arithmetic intensity, we achieve both speedup and scaling through several key innovations, three of which we highlight:

*Novel Distributed-Memory Sampling Procedures.* Random sample selection is challenging to implement when the CP factor matrices and sparse tensor are divided among  $P$  processors. We introduce two distinct communication-avoiding algorithms for randomized sample selection from the Khatri-Rao product. First, we show how to implement the CP-ARLS-LEV algorithm by computing an independent probability distribution on the factor block row owned by each processor. The resulting distributed algorithm has minimal compute / communication overhead compared to the other phases of CP decomposition. The second algorithm, STS-CP, requires higher sampling time, but achieves lower error by performing random walks on a binary tree for each sample. By distributing leaf nodes uniquely to processors and replicating internal nodes, we give a sampling algorithm with per-processor communication bandwidth scaling as  $O(\log P/P)$  (see Table 2).

*Communication-Optimized MTTKRP.* We show that communication-optimal schedules for non-randomized ALS may exhibit disproportionately high communication costs for randomized algorithms. To combat this, we use an “accumulator-stationary” schedule that eliminates expensive Reduce-scatter collectives, causing all communication costs to scale with the number of random samples taken. This alternate schedule significantly reduces communication on tensors with large dimensions (Figure 8) and empirically improves the computational load balance (Figure 11).

*Local Tensor Storage Format.* Existing storage formats developed for sparse CP decomposition [10, 20] are not optimized for random access into the sparse tensor, which our algorithms require. In response, we use a modified compressed-sparse-column format to store each matricization of our tensor, allowing efficient selection of nonzero entries by our random sampling algorithms. We then transform the selected nonzero entries into compressed sparse row format, which eliminates shared-memory data races in the subsequent sparse-dense matrix multiplication. The cost of the transposition is justified and provides a roughly 1.7x speedup over using atomics in a hybrid OpenMP / MPI implementation.

Our distributed-memory randomized algorithms have significant advantages over existing libraries while preserving the accuracy of the final approximation. As Figure 2 shows, our method d-STC-CP computes a rank 100 decomposition of the Reddit tensor ( $\sim 4.7$

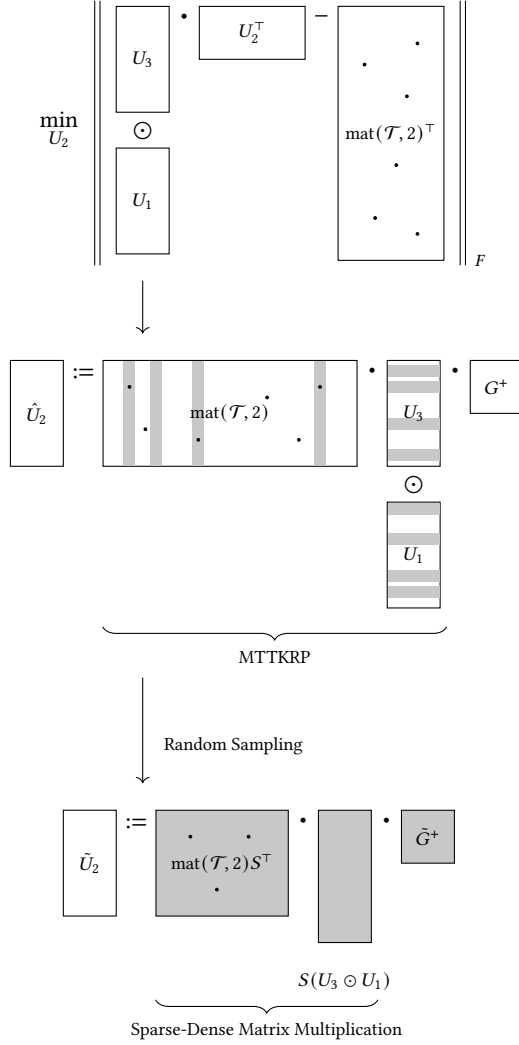


**Figure 3: Top: the linear least-squares problem to optimize factor matrix  $U_2$  during the ALS algorithm for a 3D tensor (column dimension of  $\text{mat}(\mathcal{T}, 2)$  not to scale). Middle: the exact solution to the problem using the Matricized Tensor Times Khatri-Rao Product (MTTKRP). Shaded columns of  $\text{mat}(\mathcal{T}, 2)$  and rows of  $(U_3 \odot U_1)$  are selected by our random sampling algorithm. Bottom: the downsampled linear least-squares problem after applying random sampling matrix  $S$ .**

billion nonzero entries) with a 11x speedup over SPLATT, a state-of-the-art distributed-memory CP decomposition package. The reported speedup was achieved on 512 CPU cores, with a final fit within 0.8% of non-randomized ALS for the same iteration count. While the distributed algorithm d-CP-ARLS-LEV achieves a lower final accuracy, it makes progress faster than SPLATT and spends less time on sampling (completing 80 rounds in an average of 81 seconds). We demonstrate that it is well-suited to smaller tensors and lower target ranks.

Symbol	Description
$\mathcal{T}$	Sparse tensor of dimensions $I_1 \times \dots \times I_N$
$R$	Target Rank of CP Decomposition
$U_1, \dots, U_N$	Dense factor matrices, $U_j \in \mathbb{R}^{I_j \times R}$
$\sigma$	Vector of scaling factors, $\sigma \in \mathbb{R}^R$
$J$	Sample count for randomized ALS
$\cdot$	Matrix multiplication
$\otimes$	Elementwise multiplication
$\otimes$	Kronecker product
$\odot$	Khatri-Rao product
$P$	Total processor count
$P_1, \dots, P_N$	Dimensions of processor grid, $\prod_i P_i = P$
$U_i^{(p_j)}$	Block row of $U_i$ owned by processor $p_j$

**Table 1: Symbol Definitions**

## 2 NOTATION AND PRELIMINARIES

Table 1 summarizes our notation. We use script characters (e.g.  $\mathcal{T}$ ) to denote tensors with at least three modes, capital letters for matrices, and lowercase letters for vectors. Bracketed tuples following any of these objects, e.g.  $A[i, j]$ , represent indexes into each object, and the symbol “:” in place of any index indicates a slicing of a tensor. We use  $\odot$  to denote the Khatri-Rao product, which is a column-wise Kronecker product of a pair of matrices with the same number of columns. For  $A \in \mathbb{R}^{I \times R}$ ,  $B \in \mathbb{R}^{J \times R}$ ,  $A \odot B$  produces a matrix of dimensions  $(IJ) \times R$  such that for  $1 \leq j \leq R$ ,

$$(A \odot B)[:, j] = A[:, j] \otimes B[:, j].$$

Let  $\mathcal{T}$  be an  $N$ -dimensional tensor indexed by tuples  $(i_1, \dots, i_N) \in [I_1] \times \dots \times [I_N]$ , with  $\text{nnz}(\mathcal{T})$  as the number of nonzero entries. In this work, sparse tensors are always represented as a collection of  $(N + 1)$ -tuples, with the first  $N$  elements giving the indices of a nonzero element and the last element giving the value. We seek a low-rank approximation of  $\mathcal{T}$  given by Equation (1), the right-hand-side of which we abbreviate as  $[\sigma; U_1, \dots, U_N]$ . By convention, each column of  $U_1, \dots, U_N$  has unit norm. Our goal is to minimize the sum of squared differences between our approximation and the provided tensor:

$$\text{argmin}_{\sigma, U_1, \dots, U_N} \| [\sigma; U_1, \dots, U_N] - \mathcal{T} \|_F^2. \quad (2)$$

### 2.1 Non-Randomized ALS CP Decomposition

Minimizing Equation (2) jointly over  $U_1, \dots, U_N$  is still a non-convex problem (the vector  $\sigma$  can be computed directly from the factor matrices by renormalizing each column). Alternating least squares is a popular heuristic algorithm that iteratively drives down the approximation error. The algorithm begins with a set of random factor matrices and optimizes the approximation in rounds, each involving  $N$  subproblems. The  $j$ -th subproblem in a round holds all factor matrices but  $U_j$  constant and solves for a new matrix  $\hat{U}_j$  minimizing the squared Frobenius norm error [8]. The updated matrix  $\hat{U}_j$  is the solution to the overdetermined linear least-squares problem

$$\hat{U}_j := \min_X \| U_{\neq j} \cdot X^T - \text{mat}(\mathcal{T}, j)^T \|_F. \quad (3)$$

Here, the design matrix is

$$U_{\neq j} := U_N \odot \dots \odot U_{j+1} \odot U_{j-1} \odot \dots \odot U_1,$$

which is a Khatri-Rao Product (KRP) of the factors held constant. The matrix  $\text{mat}(\mathcal{T}, j)$  is a *matricization* of the sparse tensor  $\mathcal{T}$ , which reorders the tensor modes and flattens it into a matrix of dimensions  $I_j \times (\prod_{i \neq j} I_i)$ . We solve the problem efficiently using the normal equations. Denoting the Gram matrix by  $G = (U_{\neq j})^\top (U_{\neq j})$ , we have

$$\hat{U}_j := \text{mat}(\mathcal{T}, j) \cdot U_{\neq j} \cdot G^+, \quad (4)$$

where  $G^+$  is the Moore–Penrose pseudo-inverse of  $G$ . Since  $U_{\neq j}$  is a Khatri-Rao product, we can efficiently compute  $G$  through the well-known [8] formula

$$G = \bigotimes_{k \neq j} (U_k^\top U_k), \quad (5)$$

where  $\otimes$  denotes elementwise multiplication. Figure 3 illustrates each least-squares problem, and Algorithm 1 summarizes the ALS procedure, including a renormalization of factor matrix columns after each solve. We implement the initialization step in line 1 by drawing all factor matrix entries from a unit-variance Gaussian distribution, a standard technique [6].

---

**Algorithm 1** CP-ALS( $\mathcal{T}, R$ )

---

- 1: Initialize  $U_j \in \mathbb{R}^{I_j \times R}$  randomly for  $1 \leq j \leq N$ .
  - 2: Renorm.  $U_j[:, i] \leftarrow \|U_j[:, i]\|_2, 1 \leq j \leq N, 1 \leq i \leq R$ .
  - 3: Initialize  $\sigma \in \mathbb{R}^R$  to [1].
  - 4: **while** not converged **do**
  - 5:   **for**  $j = 1 \dots N$  **do**
  - 6:      $U_j := \text{argmin}_X \|U_{\neq j} \cdot X^\top - \text{mat}(\mathcal{T}, j)^\top\|_F$
  - 7:      $\sigma[i] = \|U_j[:, i]\|_2, 1 \leq i \leq R$
  - 8:     Renorm.  $U_j[:, i] \leftarrow \|U_j[:, i]\|_2, 1 \leq i \leq R$ .
  - 9: **return**  $[\sigma; U_1, \dots, U_N]$ .
- 

The most expensive component of the ALS algorithm is the matrix multiplication  $\text{mat}(\mathcal{T}, j) \cdot U_{\neq j}$  in Equation (4), an operation known as the Matricized Tensor-Times-Khatri Rao Product (MTTKRP). For a sparse tensor  $\mathcal{T}$ , this kernel has a computational pattern similar to sparse-dense matrix multiplication (SpMM): for each nonzero in the sparse tensor, we compute a scaled Hadamard product between  $N - 1$  rows of the constant factor matrices and add it to a row of the remaining factor matrix. The MTTKRP runtime is

$$O(\text{nnz}(\mathcal{T})NR), \quad (6)$$

which is linear in the nonzero count of  $\mathcal{T}$ . Because  $\mathcal{T}$  may have billions of nonzero entries, we seek methods to drive down the cost of the MTTKRP.

## 2.2 Randomized Leverage Score Sampling

Sketching is a powerful tool to accelerate least squares problems of the form  $\min_X \|AX - B\|_F$  where  $A$  has far more rows than columns [17–19]. We apply a structured sketching matrix  $S^{J \times I}$  to both  $A$  and  $B$ , where the row count of  $S$  satisfies  $J \ll I$ . The resulting problem  $\min_{\tilde{X}} \|S(A\tilde{X} - B)\|_F$  is cheaper to solve, and the solution  $\tilde{X}$  has residual arbitrarily close (for sufficiently high  $J$ ) to the true minimum with high probability. We seek a sketching operator  $S$

with an efficiently computable action on  $A$ , which is a Khatri-Rao product.

We choose  $S$  to be a *sampling* matrix with a single nonzero per row (see Section 3.2 for alternatives). This matrix extracts and reweights  $J$  rows from both  $A$  and  $B$ , preserving the sparsity of the matricized tensor  $B$ . The cost to solve the  $j$ -th sketched sub-problem is dominated by the downsampled MTTKRP operation  $\text{mat}(\mathcal{T}, j)S^\top S U_{\neq j}$ , which has runtime

$$O(\text{nnz}(\text{mat}(\mathcal{T}, j)S^\top)NR). \quad (7)$$

As Figure 3 (bottom) illustrates,  $\text{mat}(\mathcal{T}, j)S^\top$  typically has far fewer nonzeros than  $\mathcal{T}$ , enabling sampling to reduce the computation cost in Equation (6). To select indices to sample, we implement two algorithms that involve the *leverage scores* of the design matrix [6, 13, 15]. Given a matrix  $A \in \mathbb{R}^{I \times R}$ , the leverage score of row  $i$  is given by

$$\ell_i = A[i, :] (A^\top A)^+ A[i, :]^\top. \quad (8)$$

These scores induce a probability distribution over the rows of matrix  $A$ , which we can interpret as a measure of importance. As the following theorem from Larsen and Kolda [6] (building on similar results by Mahoney and Drineas [18]) shows, sampling from either the exact or approximate distribution of statistical leverage guarantees, with high probability, that the solution to the downsampled problem has low residual with respect to the original problem.

**THEOREM 2.1 (LARSEN AND KOLDA [6]).** *Let  $S \in \mathbb{R}^{J \times I}$  be a sampling matrix for  $A \in \mathbb{R}^{I \times R}$  where each row  $i$  is sampled i.i.d. with probability  $p_i$ . Let  $\beta = \min_{i \in [I]} (p_i R / \ell_i)$ . For a constant  $C$  and any  $\epsilon, \delta \in (0, 1)$ , let the sample count be*

$$J = \frac{R}{\beta} \max \left( C \log \frac{R}{\delta}, \frac{1}{\epsilon \delta} \right).$$

Letting  $\tilde{X} = \text{argmin}_{\tilde{X}} \|SA\tilde{X} - SB\|_F$ , we have

$$\|A\tilde{X} - B\|_F^2 \leq (1 + \epsilon) \min_{\tilde{X}} \|AX - B\|_F^2.$$

with probability at least  $1 - \delta$ .

Here,  $\beta \leq 1$  quantifies deviation of the sampling probabilities from the exact leverage score distribution, with a higher sample count  $J$  required as the deviation increases. The STS-CP samples from the exact leverage distribution with  $\beta = 1$ , achieving higher accuracy at the expense of increased sampling time. CP-ARLS-LEV samples from an approximate distribution with  $\beta < 1$ .

Sketching methods for tensor decomposition have been extensively investigated [6, 13, 14, 21, 22], both in theory and practice. Provided an appropriate sketch row count  $J$  and assumptions common in the optimization literature, rigorous convergence guarantees for randomized ALS can be derived [23].

## 3 RELATED WORK

### 3.1 High-Performance ALS CP Decomposition

Significant effort has been devoted to optimizing the shared-memory MTTKRP using new data structures for the sparse tensor, cache-blocked computation, loop reordering strategies, and methods that minimize data races between threads [20, 24–29]. Likewise, several works provide high-performance algorithms for ALS CP decomposition in a distributed-memory setting. Smith and Karypis provide an

algorithm that distributes load-balanced chunks of the sparse tensor to processors in an  $N$ -dimensional Cartesian topology [16]. Factor matrices are shared among slices of the topology that require them, and each processor computes a local MTTKRP before reducing results with a subset of processors. The SPLATT library [10] implements this communication strategy and uses the compressed sparse fiber (CSF) format to accelerate local sparse MTTKRP computations on each processor.

Ballard et al. [30]. use a similar communication strategy to compute the MTTKRP involved in dense nonnegative CP decomposition. They further introduce a dimension-tree algorithm that reuses partially computed terms of the MTTKRP between ALS optimization problems. DFacTo [9] instead reformulates the MTTKRP as a sequence of sparse matrix-vector products (SpMV), taking advantage of extensive research optimizing the SpMV kernel. Smith and Karypis [16] note, however, that DFacTo exhibits significant communication overhead. Furthermore, the sequence of SpMV operations cannot take advantage of access locality within rows of the dense factor matrices, leading to more cache misses than strategies based on sparse-matrix-times-dense-matrix-multiplication (SpMM). GigaTensor [31] uses the MapReduce model in Hadoop to scale to distributed, fault-tolerant clusters. Ma and Solomonik [32] use pairwise perturbation to accelerate CP-ALS, reducing the cost of MTTKRP computations when ALS is sufficiently close to convergence using information from prior rounds.

Our work investigates variants of the Cartesian data distribution scheme adapted for a downsampled MTTKRP. We face challenges adapting either specialized data structures for the sparse tensor or dimension-tree algorithms. By extracting arbitrary nonzero elements from the sparse tensor, randomized sampling destroys the advantage conferred by formats such as CSF. Further, each least-squares solve requires a fresh set of rows drawn from the Khatri-Rao product design matrix, which prevents efficient reuse of results from prior MTTKRP computations.

Libraries such as the Cyclops Tensor Framework (CTF) [33] automatically parallelize distributed-memory contractions of both sparse and dense tensors. SpDISTAL [34] proposes a flexible domain-specific language to schedule sparse tensor linear algebra on a cluster, including the MTTKRP operation. The randomized algorithms investigated here could be implemented on top of either library, but it is unlikely that current tensor algebra compilers can automatically produce the distributed samplers and optimized communication schedules that we contribute.

### 3.2 Alternate Sketching Algorithms and Tensor Decomposition Methods

Besides leverage score sampling, popular options for sketching Khatri-Rao products include Fast Fourier Transform-based sampling matrices [35] and structured random sparse matrices (e.g. Countsketch) [21, 36]. The former method, however, introduces fill-in when applied to the sparse matricized tensor  $\text{mat}(\mathcal{T}, j)$ . Because the runtime of the downsampled MTTKRP is linearly proportional to the nonzero count of  $\text{mat}(\mathcal{T}, j)S^T$ , the advantages of sketching are lost due to fill-in. While Countsketch operators do not introduce fill, they still require access to all nonzeros of the sparse tensor

at every iteration, which is expensive when  $\text{nnz}(\mathcal{T})$  ranges from hundreds of millions to billions.

Other algorithms besides ALS exist for large sparse tensor decomposition. Stochastic gradient descent (SGD, investigated by Kolda and Hong [37]) iteratively improves CP factor matrices by sampling minibatches of indices from  $\mathcal{T}$ , computing the gradient of a loss function at those indices with respect to the factor matrices, and adding a step in the direction of the gradient to the factors. Gradient methods are flexible enough to minimize a variety of loss functions besides the Frobenius norm error [5], but require tuning additional parameters (batch size, learning rate) and a distinct parallelization strategy.

## 4 DISTRIBUTED-RANDOMIZED CP DECOMPOSITION

In this section, we distribute Algorithm 1 to  $P$  processors when random sampling is used to solve the least-squares problem on line 6. Figure 4 (left) shows the initial data distribution of our factor matrices and tensor to processors, which are arranged in a hypercube of dimensions  $P_1 \times \dots \times P_N$  with  $\prod_i P_i = P$ . Matrices  $U_1, \dots, U_N$  are distributed by block rows among the processors to ensure an even division of computation, and we denote by  $U_i^{(p_j)}$  the block row of  $U_i$  owned by processor  $p_j \in [P]$ . We impose that all processors can access the Gram matrix  $G_i$  of each factor  $U_i$ , which is computed by an Allreduce of the  $R \times R$  matrices  $U_i^{(p_j)\top} U_i^{(p_j)}$  across  $p_j \in [1, \dots, P]$ . Using these matrices, the processors redundantly compute the overall Gram matrix  $G$  through Equation (5), and by extension  $G^+$ .

With these preliminaries, each processor takes the following actions to execute steps 6-8 of Algorithm 1:

- (1) **Sampling and All-gather:** Sample rows of  $U_{\#j}$  according to the leverage-score distribution and Allgather the rows to processors who require them. For non-randomized ALS, no sampling is required.
- (2) **Local Computation:** Extract the corresponding nonzeros from the local tensor owned by each processor and execute the downsampled MTTKRP, a sparse-dense matrix multiplication.
- (3) **Reduction and Postprocessing:** Reduce the accumulator of the sparse-dense matrix multiplication across processors, if necessary, and post-process the local factor matrix slice by multiplying with  $G^+$ . Renormalize the factor matrix columns and update sampling data structures.

Multiple prior works establish the correctness of this schedule [16, 30]. We now examine strategies for drawing samples (step 1), communicating factor matrix rows (steps 2 and 3), and performing local computation efficiently (step 2) tailored to the case of randomized least-squares.

### 4.1 New Distributed Sampling Strategies

Table 2 gives the asymptotic per-processor computation and communication costs to draw  $J$  samples in our distributed versions of CP-ARLS-LEV and STS-CP. We give detailed descriptions, as well as pseudo-code, for each sampling strategy in Appendices A and B. In this section, we briefly describe the accuracy characteristics

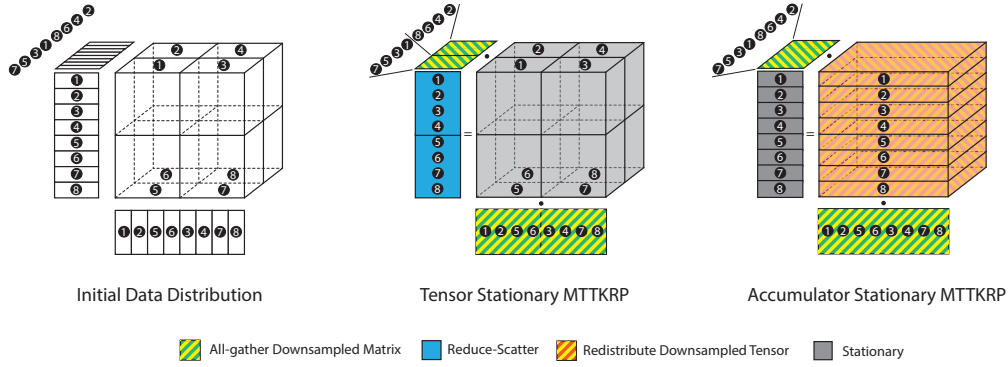


**Figure 4: Initial data distribution and downsampled MTTKRP data movement for a 3D tensor,  $P = 8$  processors. Rectangles along each side of the tensor illustrate factor matrices corresponding to each mode, divided by block rows among processors. Each black circle denotes the processor owning a block of a matrix or tensor; multiple circles on an object indicate replication of a piece of data. Colors / shading indicate communication collectives.**

Sampler	Compute	Messages	Words Sent/Recv
d-CP-ARLS-LEV	$JN/P$	$P$	$JN/P$
d-STC-CP	$(JN/P)R^2 \log P$	$NP \log P$	$(J/P)NR \log P$

**Table 2: Asymptotic Per-Processor Costs to Draw  $J$  Samples**

Schedule	Words Communicated / Round
Non-Randomized TS	$2NR \left( \prod_{k=1}^N I_k/P \right)^{1/N}$
Sampled TS	$NR \left( \prod_{k=1}^N I_k/P \right)^{1/N}$
Sampled AS	$JRN(N-1)$

**Table 3: Communication Costs for Downsampled MTTKRP**

and communication / computation patterns for each method. Table 2 does not include the costs to construct the sampling data structures in each algorithm, which are subsumed asymptotically by the matrix-multiplication  $U_i^{(p_j)} \cdot G^+$  on each processor (step 3). The costs of all communication collectives are taken from Chan et al. [38].

**CP-ARLS-LEV:** The CP-ARLS-LEV algorithm by Larsen and Kolda [6] approximates the leverage scores in Equation (8) by the product of leverage scores for each factor matrix  $U_1, \dots, U_N$ . The leverage scores of the block row  $U_i^{(p_j)}$  owned by processor  $p_j$  are approximated by

$$\tilde{\ell}^{(p_j)} = \text{diag} \left( U_i^{(p_j)} G_i^+ U_i^{(p_j)\top} \right)$$

which, given the replication of  $G_i^+$ , can be constructed independently by each processor in time  $O(R^2 I_i/P)$ . The resulting probability vector, which is distributed among  $P$  processors, can be sampled in expected time  $O(J/P)$ , assuming that the sum of leverage scores distributed to each processor is roughly equal (see Section 4.4 on

load balancing for methods to achieve this). Multiplying by  $(N-1)$  to sample independently from each matrix held constant, we get an asymptotic computation cost  $O(JN/P)$  for the sampling phase. Processors exchange only a constant multiple of  $P$  words to communicate the sum of leverage scores that they hold locally and the exact number of samples they must draw, as well as a cost  $O(JN/P)$  to evenly redistribute / postprocess the final sample matrix. While this algorithm is computationally efficient, it requires  $J = \tilde{O}(R^{N-1}/(\epsilon\delta))$  to achieve the  $(\epsilon, \delta)$ -guarantee from Theorem 2.1, which may lead to a higher runtime in the distributed-memory MTTKRP. Larsen and Kolda note that CP-ARLS-LEV sampling can be implemented without any communication at all if an entire factor matrix is assigned uniquely to a single processor, which can compute leverage scores and draw samples independently [6]. That said, assigning an entire factor matrix to a single processor incurs higher communication costs in the MTTKRP phase of the algorithm and may be infeasible under tight memory constraints, leading to our adoption of a block-row distribution for the factors.

**STS-CP:** The STS-CP algorithm [15] samples from the exact leverage distribution by executing a random walk on a binary tree data structure once for each of the  $N-1$  factor matrices held constant. Each leaf of the binary tree corresponds to a block of  $R$  rows from a factor matrix  $U_i$  and holds the  $R \times R$  Gram matrix of that block row. Each internal node  $v$  holds a matrix  $G^v$  that is the sum of the matrices held by its children. Each sample begins with a unique vector  $h$  at the root of the tree. At each non-leaf node  $v$ , the algorithm computes  $(h^\top G^{L(v)} h) / (h^\top G^v h)$ . If this quantity is greater than a random number  $r$  unique to each sample, the algorithm sends the sample to the left subtree, and otherwise the right subtree. The process repeats until the random walk reaches a leaf and a row index is selected.

We distribute the data structure and the random walk as shown in Figure 5. We assume that  $P$  is a power of two to simplify our description, but our implementation makes no such restriction. Each processor  $p_j$  owns a subtree of the larger tree that corresponds to their block row  $U_i^{(p_j)}$ . The roots of these subtrees all occur at the same depth  $L = \log P$ . Above level  $L$ , each node stores  $2 \log P$



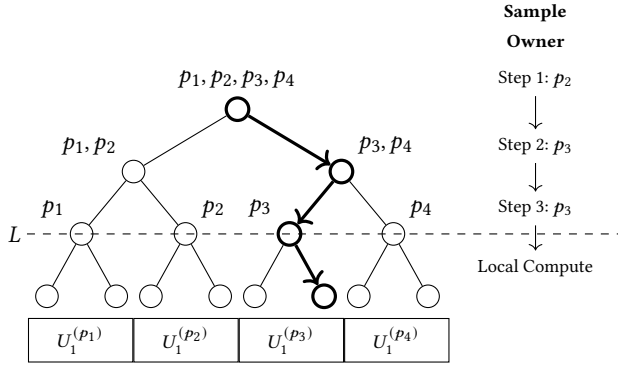


**Figure 5: Example random walk in STS-CP to draw a single sample index from matrix  $U_1$ , distributed to  $P = 4$  processors. Annotations on the tree (left) indicate processors that share data for each node. The schedule to the right indicates the processor that owns the sample at each stage of the random walk. The sample begins randomly at  $p_2$ , then branches left to  $p_3$  ( $p_4$  shares node data and could also have been selected), involving communication of a vector corresponding to the sample from  $p_2$  to  $p_3$ . The sample remains at  $p_3$  for the remainder of the walk.**

additional matrices,  $G^v$  and  $G^{L(v)}$ , for each ancestor node  $v$  of its subtree.

To execute the random walks, each sample is assigned randomly to a processor which evaluates the branching threshold at the tree root. Based on the direction of the branch, the sample and corresponding vector  $h$  are routed to a processor that owns the required node information, and the process repeats until the walk reaches level  $L$ . The remaining steps do not require communication.

The replication of node information above level  $L$  requires communication overhead  $O(R^2 \log P)$  using the classic bi-directional exchange algorithm for Allreduce [38]. For a batch of  $J$  samples, each level of the tree requires  $O(JR^2)$  FLOPs to evaluate the branching conditions. Under the assumption that the final sampled rows are distributed evenly to processors, the computation and communication at each level are load balanced in expectation. Each processor has expected computation cost  $O((J/P)NR^2 \log P)$  over all levels of the tree and all matrices  $U_i$ ,  $1 \leq i \leq N$ ,  $i \neq k$ . Communication of samples between tree levels is accomplished through All-to-allv collective calls, requiring  $O(NP \log P)$  messages and  $O((J/P)NR \log P)$  words sent / received in expectation by each processor.

## 4.2 A Randomization-Tailored MTTKRP Schedule

The goal of this section is to demonstrate that an optimal communication schedule for non-randomized ALS may incur unnecessary overhead for the randomized algorithm. In response, we will use a schedule where all communication costs scale with the number of random samples taken, enabling the randomized algorithm to decrease *communication costs* as well as computation. Table 3 gives

lower bounds on the communication required for each schedule we consider, and we derive the exact costs in this section.

The two schedules that we consider are “tensor-stationary”, where factor matrix rows are gathered and reduced across a grid, and “accumulator-stationary”, where no reduction takes place. These distributions were compared by Smith and Karypis [16] under the names “medium-grained” and “course-grained”, respectively. Both distributions exhibit, under an even distribution of tensor nonzero entries and leverage scores to processors, ideal expected computation scaling. Therefore, we focus our analysis on communication. We begin by deriving the communication costs for non-randomized ALS under the tensor-stationary communication schedule, which we will then adapt to the randomized case.

Although our input tensor is sparse, we model the **worst-case** communication costs for the dense factor matrices with standard Allgather and Reduce-scatter primitives. For non-randomized (exact) ALS, the cost we derive matches that given by Smith and Karypis in their sparse tensor decomposition work [16]. Furthermore consider the extremely sparse Reddit tensor, (nonzero fraction  $4 \times 10^{-10}$  [1]), which nonetheless exhibits an average of 571 nonzeros per fiber along the longest tensor mode and an average of 26,000 nonzeros per fiber aligned with the shortest tensor mode. The high per-fiber nonzero count induces a practical communication cost comparable to the worst-case bounds, a feature that Reddit shares with other datasets in Table 4.

**Exact Tensor-Stationary:** The tensor-stationary MTTKRP algorithm is communication-optimal for dense CP decomposition [30] and outperforms several other methods in practice for non-randomized sparse CP decomposition. [16]. The middle image of Figure 4 illustrates the approach. During the  $k$ -th optimization problem in a round of ALS, each processor does the following:

- (1) For any  $i \neq k$ , participates in an Allgather of all blocks  $U_i^{(p_j)}$  for all processors  $p_j$  in a slice of the processor grid aligned with mode  $k$ .
- (2) Executes an MTTKRP with locally owned nonzeros and the gathered row blocks.
- (3) Executes a Reduce-scatter with the MTTKRP result along a slice of the processor grid aligned with mode  $j$ , storing the result in  $U_k^{(p_j)}$

For non-randomized ALS, the gather step must only be executed once per round and can be cached. Then the communication cost for the All-gather and Reduce-scatter collectives summed over all  $k = 1 \dots N$  is

$$2 \sum_{k=1}^N I_k R / P_k.$$

To choose the optimal grid dimensions  $P_k$ , we minimize the expression above subject to the constraint  $\prod_{k=1}^N P_k = P$ . Straightforward application of Lagrange multipliers leads to the optimal grid dimensions

$$P_k = I_k \left( P / \prod_{i=1}^N I_i \right)^{1/N}.$$

These are the same optimal grid dimensions reported by Ballard et al. [30]. The communication under this optimal grid is

$$2NR \left( \prod_{k=1}^N I_k / P \right)^{1/N}.$$

**Downsampled Tensor-Stationary:** As Figure 4 illustrates, only factor matrix rows that are selected by the random sampling algorithm need to be gathered by each processor in randomized CP decomposition. Under the assumption that sampled rows are evenly distributed among the processors, the expected cost of gathering rows reduces to  $JR(N-1)/P_k$  within slices along mode  $k$ . The updated communication cost under the optimal grid dimensions derived previously is

$$\frac{R \left( \prod_{k=1}^N I_k \right)^{1/N}}{P^{1/N}} \left[ N + \sum_{k=1}^N \frac{J(N-1)}{I_k} \right].$$

The second term in the bracket arises from Allgather collectives of sampled rows, which is small if  $J \ll I_k$  for all  $1 \leq k \leq N$ . The first term in the bracket arises from the Reduce-scatter, which is unchanged by the sampling procedure. Ignoring the second term in the expression above gives the second entry of Table 3.

Observe that this randomized method spends the same time on the reduction as the non-randomized schedule while performing significantly less computation, leading to diminished arithmetic intensity. On the other hand, this distribution may be optimal when the tensor dimensions  $I_k$  are small or the sample count  $J$  is high enough.

**Downsampled Accumulator-Stationary:** As shown by Smith and Karypis [16], the accumulator-stationary data distribution performs poorly for non-randomized ALS. In the worst case, each processor requires access to all entries from all factors  $U_1, \dots, U_N$ , leading to high communication and memory overheads. On the other hand, we demonstrate that this schedule may be optimal for *randomized* ALS on tensors where the sample count  $J$  is much smaller than the tensor dimensions. The rightmost image in Figure 4 illustrates the approach, which avoids the expensive Reduce-scatter collective. To optimize  $U_k$ , we keep the destination buffer for a block row of  $U_k$  stationary on each processor while communicating only sampled factor matrix rows and nonzeros of  $\mathcal{T}$ . Under this distribution, all sampled factor matrix rows must be gathered to all processors. The cost of the gather step for a single round becomes  $O(JRN(N-1))$  (for each of  $N$  least-squares problems, we gather at most  $J(N-1)$  rows of length  $R$ ). Letting  $S_1, \dots, S_N$  be the sampling matrices for each ALS subproblem in a round, the number of nonzeros selected in problem  $j$  is  $\text{nnz}(\text{mat}(\mathcal{T}, j)S_j)$ . These selected (row, column, value) triples must be redistributed as shown in Figure 4 via an All-to-allv collective call. Assuming that the source and destination for each nonzero are distributed uniformly among the processors, the expected cost of redistribution in least-squares problem  $j$  is  $(3/P)\text{nnz}(\text{mat}(\mathcal{T}, j)S_j^\top)$ . The final communication cost is

$$JRN(N-1) + \frac{3}{P} \sum_{j=1}^N \text{nnz}(\text{mat}(\mathcal{T}, j)S_j^\top). \quad (9)$$

The number of nonzeros sampled varies from tensor to tensor even when the sample count  $J$  is constant. That said, the redistribution exhibits perfect scaling (in expectation) with the processor count  $P$ . In practice, we avoid redistributing the tensor entries multiple times by storing  $N$  different representations of the tensor aligned with each slice of the processor grid, a technique that competing

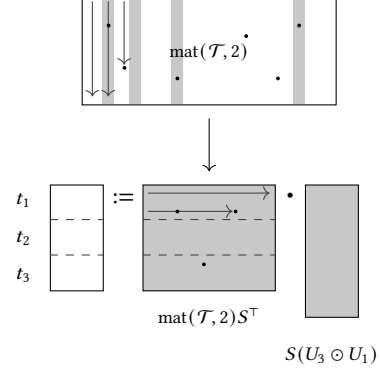


**Figure 6: Shared-memory parallelization of downsampled MTTKRP procedure. Nonzero sparse coordinates in the sampled gray columns, initially sorted by column, are selected and remapped into a CSR matrix. The subsequent matrix multiplication is parallelized to threads  $t_1, t_2, t_3$  without atomic operations or data races, since each thread is responsible for a unique block of the output.**

packages (e.g. DFacto [9], early versions of SPLATT [24]) also employ. This optimization eliminates the second term in Equation (9), giving the communication cost in the third row of Table 3. More importantly, observe that all communication scales linearly with the sample count  $J$ , enabling sketching to improve *both* the communication and computation efficiency of our algorithm. On the other hand, the term  $JRN(N-1)$  does not scale with  $P$ , and we expect that gathering rows becomes a communication bottleneck for high processor counts.

### 4.3 Tensor Storage and Local MTTKRP

As mentioned in Section 4.2, we store different representations of the sparse tensor  $\mathcal{T}$  across the processor grid to decrease communication costs. Each corresponds to a distinct matricization  $\text{mat}(\mathcal{T}, j)$  for  $1 \leq j \leq N$  used in the MTTKRP (see Figure 3). For non-randomized ALS, a variety of alternate storage formats have been proposed to reduce the memory overhead and accelerate the local computation. Smith and Karypis support a compressed sparse fiber format for the tensor in SPLATT [10, 24], and Nisa et al. [20] propose a mixed-mode compressed sparse fiber format as an improvement. These optimizations cannot improve the runtime of our randomized algorithms because they are not conducive to sampling random nonzeros from  $\mathcal{T}$ .

Instead, we adopt the approach shown in Figure 6. The coordinates in each tensor matricization are stored in sorted order of their column indices, an analogue of compressed-sparse-column (CSC) format. With this representation, the random sampling algorithm efficiently selects columns of  $\text{mat}(\mathcal{T}, j)$  corresponding to rows of the design matrix. The nonzeros in these columns are extracted and remapped to a compressed sparse row (CSR) format through a “sparse transpose” operation. The resulting CSR matrix participates in the sparse-dense matrix multiplication, which can be efficiently parallelized without data races on a team of shared-memory threads.



Tensor	Dimensions	NNZ	Prep.
Uber	$183 \times 24 \times 1.1K \times 1.7K$	3.3M	-
Amazon	$4.8M \times 1.8M \times 1.8M$	1.7B	-
Patents	$46 \times 239K \times 239K$	3.6B	-
Reddit	$8.2M \times 177K \times 8.1M$	4.7B	log

**Table 4: Sparse Tensor Datasets**

#### 4.4 Load Balance

To ensure load balance among processors, we randomly permute the sparse tensor indices along each mode, a technique also used by SPLATT [16]. These permutations ensure that each processor holds, in expectation, an equal fraction of nonzero entries from the tensor and an equal fraction of sampled nonzero entries. For highly-structured sparse tensors, random permutations do not optimize processor-to-processor communication costs, which packages such as Hypertensor [11] minimize through hypergraph partitioning. As Smith and Karypis [16] demonstrate empirically, hypergraph partitioning is slow and memory-intensive on large tensors. Because our randomized implementations require just minutes on massive tensors to produce decompositions comparable to non-randomized ALS, the overhead of partitioning outweighs the modest communication reduction it may produce.

## 5 EXPERIMENTS

Experiments were conducted on CPU nodes of NERSC Perlmutter, a Cray HPE EX supercomputer. Each node has 128 physical cores divided between two AMD EPYC 7763 (Milan) CPUs. Nodes are linked by an HPE Slingshot 11 interconnect.

Our implementation is written in C++ and links with OpenBLAS 0.3.21 for dense linear algebra. We use a simple Python wrapper around the C++ implementation to facilitate benchmarking. We use a hybrid of MPI message-passing and OpenMP shared-memory parallelism in our implementation, which is available online at [https://github.com/vbharadwaj-bk/rdist\\_tensor](https://github.com/vbharadwaj-bk/rdist_tensor).

Our primary baseline is the SPLATT, the Surprisingly Parallel Sparse Tensor Toolkit [10, 16]. SPLATT is a scalable CP decomposition package optimized for both communication costs and local MTTKRP performance through innovative sparse tensor storage structures. As a result, it remains one of the strongest libraries for sparse tensor decomposition in head-to-head benchmarks against other libraries [20, 29, 39]. We used the default medium-grained algorithm in SPLATT and adjusted the OpenMP thread count for each tensor to achieve the best possible performance to compare against.

Table 4 lists the sparse tensors used in our experiments, all sourced from the Formidable Repository of Open Sparse Tensors and Tools (FROSTT) [1]. Besides Uber, which was only used to verify accuracy due to its small size, the Amazon, Patents, and Reddit tensors are the only members of FROSTT at publication time with over 1 billion nonzero entries. These tensors were identified to benefit the most from randomized sampling since the next largest tensor in the collection, NELL-1, has 12 times fewer nonzeros than

Tensor	$R$	d-CP-ARLS-LEV	d-STS-CP	Exact
Uber	25	0.187	0.189	0.190
	50	0.211	0.216	0.218
	75	0.218	0.230	0.232
Amazon	25	0.338	0.340	0.340
	50	0.359	0.366	0.366
	75	0.368	0.381	0.382
Patents	25	0.451	0.451	0.451
	50	0.467	0.467	0.467
	75	0.475	0.475	0.476
Reddit	25	0.0583	0.0592	0.0596
	50	0.0746	0.0775	0.0783
	75	0.0848	0.0910	0.0922

**Table 5: Average Fits,  $J = 2^{16}$ , 32 MPI Ranks, 4 Nodes**

Amazon. We computed the logarithm of all values in the Reddit tensor, consistent with established practice [6].

### 5.1 Correctness at Scale

Table 5 gives the average fits (5 trials) of decompositions produced by our distributed-memory algorithms. The fit [6] between the decomposition  $\tilde{\mathcal{T}} = [\sigma; U_1, \dots, U_N]$  and the ground-truth  $\mathcal{T}$  is defined as

$$\text{fit}(\tilde{\mathcal{T}}, \mathcal{T}) = 1 - \frac{\|\tilde{\mathcal{T}} - \mathcal{T}\|_F}{\|\mathcal{T}\|_F}.$$

A fit of 1 indicates perfect agreement between the decomposition and the input tensor. We used  $J = 2^{16}$  for our randomized algorithms to test our implementations on configurations identical to those in prior work [6, 15]. To test both the distributed-memory message passing and shared-memory threading parts of our implementation, we used 32 MPI ranks and 16 threads per rank across 4 CPU nodes. We report accuracy for the accumulator-stationary versions of our algorithms and checked that the tensor-stationary variants produced the same mean fits. The ‘‘Exact’’ column gives the fits generated by SPLATT. ALS was run for 40 rounds on all tensors except Reddit, for which we used 80 rounds.

The accuracy of both d-CP-ARLS-LEV and d-STS-CP match the shared-memory prototypes in the original works [6, 15]. As theory predicts, the accuracy gap between d-CP-ARLS-LEV and d-STS-CP widens at higher rank. The fits of our methods improves by increasing the sample count  $J$  at the expense of higher sampling and MTTKRP runtime.

### 5.2 Speedup over Baselines

Figure 7 shows the speedup of our randomized distributed algorithm per ALS round over SPLATT at 4 nodes and 16 nodes. We used the same configuration and sample count for each tensor as Table 5. On Amazon and Reddit at rank 25 and 4 nodes, d-STS-CP achieves a speedup in the range 5.7x-6.8x while d-CP-ARLS-LEV achieves between 8.0-9.5x. We achieve our most dramatic speedup at rank

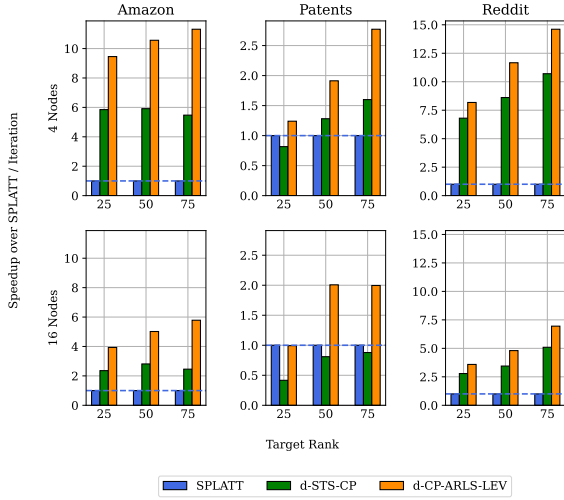


Figure 7: Average speedup per ALS iteration of our distributed randomized algorithms over SPLATT (5 trials,  $J = 2^{16}$ ).

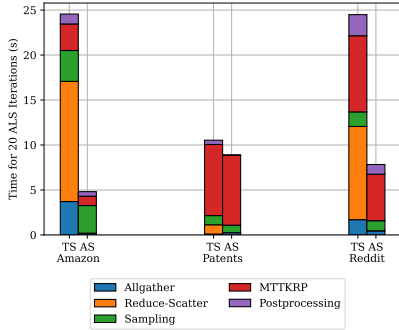


Figure 8: Average runtime (5 trials,  $R = 25$ ) per activity for tensor-stationary and accumulator-stationary distributions with 32 MPI ranks over 4 nodes.

75 on the Reddit tensor, with d-STS-CP achieving 10.7x speedup and d-CP-ARLS-LEV achieving 14.6x. Our algorithms achieve less speedup compared to SPLATT on the denser Patents tensor. Here, a larger number nonzeros are selected by randomized sampling, with a significant computation bottleneck in the step that extracts and reindexes the nonzeros from the tensor. The bottom half of Figure 7 shows that d-STS-CP maintains at least a 2x speedup over SPLATT even at 16 nodes / 2048 CPU cores on Amazon and Reddit, but exhibits worse speedup on the Patents tensor. Table 5 quantifies the accuracy sacrificed for the speedup, which can be changed by adjusting the sample count at each least-squares solve. As Figure 2 shows, both of our randomized algorithms make faster progress than SPLATT, with d-STS-CP producing a comparable rank-100 decomposition of the Reddit tensor in under two minutes.

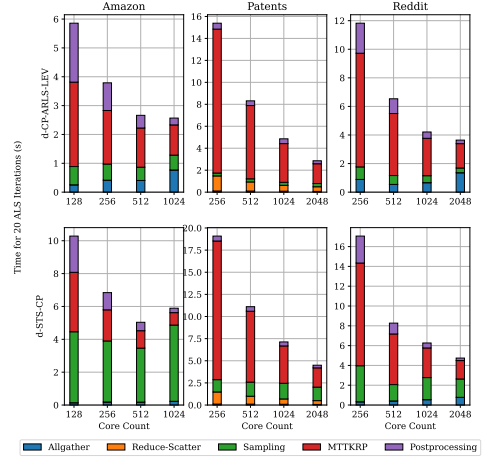


Figure 9: Average runtime (5 trials) per activity vs. CPU core count,  $R = 25$ . Each node has 128 CPU cores, and 8 MPI ranks were used per node.

### 5.3 Comparison of Communication Schedules

Figure 8 breaks down the runtime per phase of the d-STS-CP algorithm for the tensor-stationary and accumulator-stationary schedules on 4 nodes. To illustrate the effect of sampling on the row gathering step, we gather all rows (not just those sampled) for the tensor-stationary distribution, a communication pattern identical to SPLATT. Observe that the Allgather collective under the accumulator-stationary schedule is significantly cheaper for Amazon and Reddit, since only sampled rows are communicated. As predicted, the Reduce-scatter collective accounts for a significant fraction of the runtime for the tensor-stationary distribution on Amazon and Reddit, which have tensor dimensions in the millions. On both tensors, the runtime of this collective is greater than the time required by all other phases combined in the accumulator-stationary schedule. By contrast, both schedules perform comparably on Patents. Here, the Reduce-scatter cost is marginal due to the smaller dimensions of the tensor.

We conclude that sparse tensors with large dimensions can benefit from the accumulator-stationary distribution to reduce communication costs, while the tensor-stationary distribution is optimal for tensors with higher density and smaller dimensions. The difference in MTTKRP runtime between the two schedules is further explored in Section 5.6.

### 5.4 Strong Scaling and Runtime Breakdown

Figure 9 gives the runtime breakdown for our algorithms at varying core counts. Besides the All-gather and Reduce-scatter collectives used to communicate rows of the factor matrices, we benchmark time spent in each of the three phases identified in Section 4: sample identification, execution of the downsampled MTTKRP, and post-processing factor matrices.

With its higher density, the Patents tensor has a significantly larger fraction of nonzeros randomly sampled at each linear least-squares solve. As a result, most ALS runtime is spent on the downsampled MTTKRP. The Reddit and Amazon tensors, by contrast,

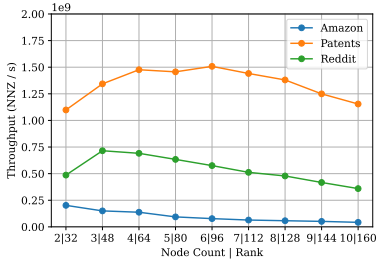


**Figure 10: Average throughput (3 trials per data point) of the d-STS-CP algorithm vs. increasing node count and rank, measured as the average number of nonzeros iterated over in the MTTKRP per second of total algorithm runtime (higher is better). Ideal scaling is a horizontal line. The ratio of node count to rank was kept constant at 16. d-STS-CP was chosen to preserve decomposition accuracy at high ranks.**

spend a larger runtime portion on sampling and post-processing the factor matrices due to their larger mode sizes. Scaling beyond 1024 cores for the Amazon tensor is impeded by the relatively high sampling cost in d-STS-CP, a consequence of repeated All-to-allv collective calls. The high sampling cost is because the Amazon tensor has side-lengths in the millions along all tensor modes, leading to deeper trees for the random walks in STS-CP.

### 5.5 Weak Scaling with Target Rank

We measure weak scaling for our randomized algorithms by recording the throughput (nonzero entries processed in the MTTKRP per second of total algorithm runtime) as both the processor count and target rank  $R$  increase proportionally. We keep the ratio of node count to rank  $R$  constant at 16. We use a fixed sample count  $J = 2^{16}$ , and we benchmark the d-STS-CP algorithm to ensure minimal accuracy loss as the rank increases.

Although the FLOP count of the MTTKRP is linearly proportional to  $R$  (see Equation (6)), we expect the efficiency of the MTTKRP to *improve* with increased rank due to spatial cache access locality in the longer factor matrix rows, a well-documented phenomenon [40]. On the other hand, the sampling runtime of the d-STS-CP algorithm grows quadratically with the rank  $R$  (see Table 2). The net impact of these competing effects is determined by the density and dimensions of the sparse tensor.

Figure 10 shows the results of our weak scaling experiments. Because ALS on the Amazon tensor spends a large fraction of time drawing samples (see Figure 9), its throughput suffers with increasing rank due to the quadratic cost of sampling. At the other extreme, our algorithm spends little time sampling from the Patents tensor with its smaller dimensions, enabling throughput to increase due to higher cache spatial locality in the factor matrices. The experiments on Reddit follow a middle path between these extremes, with performance dropping slightly at high rank due to the cost of sampling.

### 5.6 Load Imbalance

Besides differences in the communication times of the tensor-stationary and accumulator-stationary schedules, Figure 8 indicates a runtime

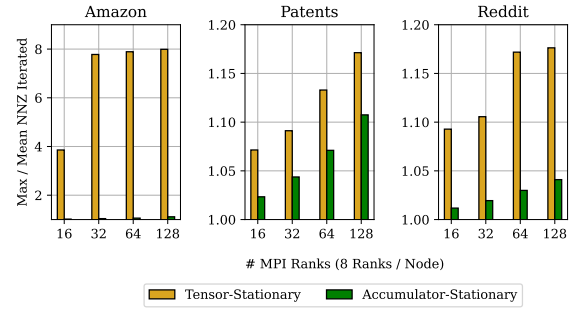


**Figure 11: Avg. Load imbalance, defined as maximum / mean nonzeros iterated over by any MPI process, for d-STS-CP. 8 MPI Ranks / Node, 5 Trials.**

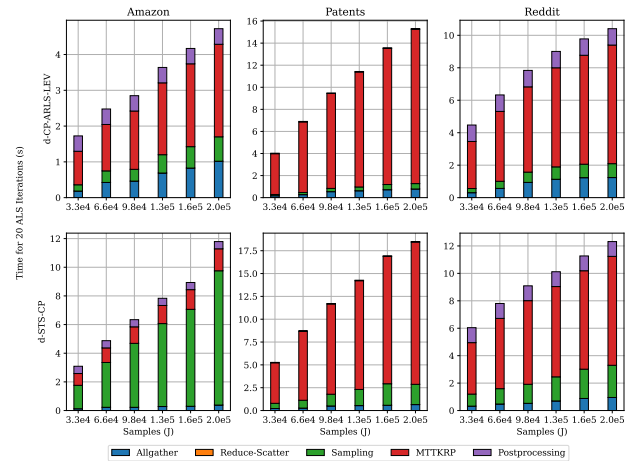


**Figure 12: Runtime breakdown vs. sample count,  $R = 25$ . 512 CPU cores, 5 trials, accumulator-stationary distribution.**

difference in the downsampled MTTKRP between the two schedules. Figure 11 offers an explanation by comparing the load balance of these methods. We measure load imbalance (averaged over 5 trials) as the maximum number of nonzeros processed in the MTTKRP by any MPI process over the mean of the same quantity.

The accumulator-stationary schedule yields better load balance over all tensors, with a dramatic difference for the case of Amazon. The latter exhibits a few rows of the Khatri-Rao design matrix with high statistical leverage and corresponding fibers with high nonzero counts, producing the imbalance. The accumulator-stationary distribution (aided by the load balancing random permutation) distributes the nonzeros in each selected fiber across all  $P$  processors, correcting the imbalance.

### 5.7 Impact of Sample Count

In prior sections, we used the sample count  $J = 2^{16}$  to establish a consistent comparison with prior work. Figure 12 demonstrates the runtime impact of increasing the sample count for both of our algorithms on all three tensors. For all experiments but one, the MTTKRP component of the runtime increases the most as  $J$  gets

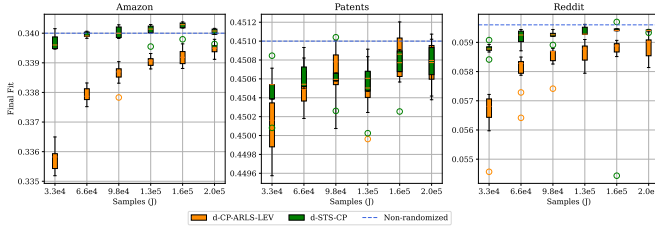


**Figure 13: Final fit of randomized CP decomposition for varying sample count  $J$ . Horizontal dashed lines indicate the fit produced by SPLATT. ALS was run for 40 iterations on Amazon and Patents, 80 iterations on Reddit, and for 10 trials each. All other experimental configuration is identical to Figure 12.**

larger. For d-STs-CP on the Amazon tensor, the runtime increase owes primarily to the higher cost of sample selection. The higher sampling time for d-STs-CP on Amazon is explained in Section 5.4. Figure 13 gives the final fits after running our randomized algorithms for varying sample counts. The increase in accuracy is minimal beyond  $J = 2^{16}$  for d-STs-CP on Amazon and Reddit. Both algorithms perform comparably on Patents. These plots suggest that sample count as low as  $J = 2^{16}$  is sufficient to achieve competitive performance with libraries like SPLATT on large tensors.

## 6 CONCLUSIONS AND FURTHER WORK

We have demonstrated in this work that randomized CP decomposition algorithms are competitive at the scale of thousands of CPU cores with state-of-the-art, highly-optimized non-randomized libraries for the same task. Future work includes improving the irregular communication pattern of the d-STs-CP algorithm, as well as deploying our algorithm on massive real-world tensors larger than those offered by FROSTT.

## 7 ACKNOWLEDGEMENTS AND FUNDING

We thank the referees for valuable feedback which helped improve the paper. V. Bharadwaj was supported by the U.S. Department of Energy, Office of Science, Office of Advanced Scientific Computing Research, Department of Energy Computational Science Graduate Fellowship under Award Number DE-SC0022158. O. A. Malik and A. Buluç were supported by the Office of Science of the DOE under Award Number DE-AC02-05CH11231. R. Murray was supported by Laboratory Directed Research and Development (LDRD) funding from Berkeley Lab, provided by the Director, Office of Science, of the U.S. DOE under Contract No. DE-AC02-05CH11231. R. Murray was also funded by an NSF Collaborative Research Framework under NSF Grant Nos. 2004235 and 2004763. This research used resources of the National Energy Research Scientific Computing Center, a DOE Office of Science User Facility, using NERSC award ASCR-ERCAP0024170.

## A DISTRIBUTED CP-ARLS-LEV SAMPLING

Let  $i_1, \dots, i_{N-1}$  denote row indices from factor matrices  $U_1, \dots, U_{N-1}$  that uniquely identify a row from the Khatri-Rao product  $U_{\neq N}$ . To efficiently sample according to an *approximate leverage score*

*distribution* on the rows of  $U_{\neq N}$ , the CP-ARLS-LEV algorithm by Larsen and Kolda [6] weights each row by

$$\tilde{\ell}_{i_1, \dots, i_{N-1}} := \prod_{k=1}^{N-1} U_k [i_k, :] G_k^+ U_k [i_k, :]^\top$$

where  $G_k := U_k^\top U_k$  for all  $k$ . Because each weight in the distribution above is a product of scores from each factor, we can draw  $i_1, \dots, i_{N-1}$  independently and concatenate the indices to assemble one row sample. Given that the factors are distributed by block rows among processors, the main challenge is to sample without gathering the probability weight vector for each  $U_k$  to a single processor.

---

### Algorithm 2 CP-ARLS-LEV-build ( $U_i^{(p_j)}$ )

---

- 1:  $G_i := \text{Allreduce} \left( U_i^{(p_j)\top} U_i^{(p_j)} \right)$
  - 2:  $\text{dist}_i^{(p_j)} := \text{diag} \left( U_i^{(p_j)} G_i^+ U_i^{(p_j)\top} \right)$
  - 3:  $C_i^{(p_j)} := \left\| \text{dist}_i^{(p_j)} \right\|_1$
  - 4:  $\text{dist}_i^{(p_j)} / = C_i^{(p_j)}$
  - 5: **Postcondition:**  $G_i^+$ ,  $\text{dist}_i^{(p_j)}$ , and  $C_i^{(p_j)}$  are initialized on each processor.
- 

Algorithms 2 and 3 give full procedures to build the distributed CP-ARLS-LEV data structure and draw samples from it, respectively. The build algorithm is called for all  $U_i$ ,  $1 \leq i \leq N$ , before the ALS algorithm begins. It is also called each time a matrix  $U_i$  is updated in an ALS round. Each procedure is executed synchronously by all processors  $p_j$ ,  $1 \leq j \leq P$ . Recall further that we define  $U_i^{(p_j)}$  as the block row of the  $i$ -th factor matrix uniquely owned by processor  $p_j$ . Algorithm 2 allows all processors to redundantly compute the Gram matrix  $G_i$  and the normalized local leverage score distribution on the block row  $U_i^{(p_j)}$ .

Algorithm 3 enables each processor to draw samples from the Khatri-Rao product  $U_{\neq k}$ . For each index  $i \neq k$ , each processor determines the fraction of  $J$  rows drawn from its local block using a consistent multinomial sample according to the weights  $C_i^{(p_j)}$ ,  $1 \leq j \leq P$ . By *consistent*, we mean that each processor executes the multinomial sampling using a pseudorandom number generator with a common seed that is shared among all processors. The result of this operation is a vector  $SC^{\text{loc}} \in \mathbb{Z}^P$  which gives the sample count each processor should draw locally. Each processor then samples from its local distribution. At the end of the algorithm, each row of  $X$  contains a sample drawn according to the approximate leverage score distribution.

We note that the sampling algorithm, as presented, involves the Allgather of a  $J \times N$  sampling matrix followed by a random permutation. We use this procedure in our code, since we found that the communication cost  $O(JN)$  was negligible for the range of sample counts we used. However, this cost can be reduced to  $O(JN/P)$ , in expectation, with an All-to-allv communication pattern that permutes the indices without gathering them to a single processor.

**Algorithm 3** CP-ARLS-LEV-sample ( $k, J$ )

---

```

1: Require: Vectors  $\text{dist}_i^{(p_j)}$ , and normalization constants  $C_i^{(p_j)}$ .
2: Initialize sample matrix  $X \in \mathbb{Z}^{J \times N}$  on all processors.
3: for  $i = 1 \dots N, i \neq k$  do
4:    $C := \text{Allgather} \left( C_i^{(p_j)} \right)$ 
5:    $W = \sum_{\ell=1}^P C[\ell]$ 
6:    $SC^{\text{loc}} := \text{consistent-multinomial}([C[1]/W, \dots, C[P]/W], J)$ 
7:    $\text{samples}^{\text{loc}} := \text{sample} \left( \text{dist}_i^{(p_j)}, SC^{\text{loc}}[j] \right)$ 
8:    $X[:, i] := \text{Allgather} \left( \text{samples}^{\text{loc}} \right)$  //See note
9:   Perform a consistent random permutation of  $X[:, i]$ 
10: return  $X$ , a set of samples from the Khatri-Rao product  $U_{\neq k}$ .

```

---

**B DISTRIBUTED STS-CP SAMPLING**

We use the same variables defined at the beginning of Appendix A. To draw samples from the *exact leverage score distribution*, the STS-CP algorithm conditions each row index draw  $i_k$  on draws  $i_1, \dots, i_{k-1}$  [15]. To formalize this, let  $\hat{i}_1, \dots, \hat{i}_{N-1}$  be random variables for each index that jointly follow the exact leverage distribution. Suppose we have already sampled  $\hat{i}_1 = i_1, \dots, \hat{i}_{k-1} = i_{k-1}$ , and let  $h = \bigotimes_{j=1}^{k-1} U_j [i_j, :]^T$  be the product of these sampled rows. Bharadwaj et. al. show that the conditional probability of  $\hat{i}_k = i_k$  is

$$p(\hat{i}_k = i_k \mid \hat{i}_{<k} = i_{<k}) \propto (U_k [i_k, :]^T \otimes h)^T G_{>k} (U_k [i_k, :]^T \otimes h)$$

where  $G_{>k} = G^+ \otimes \bigotimes_{j=k}^{N-1} G_j$  [15]. The STS-CP algorithm exploits this formula to efficiently sample from the exact leverage distribution.

Algorithms 4 and 5 give procedures to build and sample from the distributed data structure for STS-CP, which are analogues of Algorithms 2 and 3 for CP-ARLS-LEV. To simplify our presentation, we assume that the processor count  $P$  is a power of two. The general case is a straightforward extension (see Chan et. al. [38]), and our implementation makes no restriction on  $P$ . The build procedure in Algorithm 4 computes the Gram matrix  $G_i$  for each matrix  $U_i$  using a the bidirectional exchange algorithm for Allreduce [38]. The difference is that each processor caches the intermediate matrices that arise during the reduction procedure, each uniquely identified with internal nodes of the binary tree in Figure 5.

In the sampling algorithm, the cached matrices are used to determine the index of a row drawn from  $U_i$  via binary search. The matrix of sample indices  $X$  and sampled rows  $H$  are initially distributed by block rows among processors. Then for each matrix  $U_i, i \neq k$ , a random number is drawn uniformly in the interval  $[0, 1]$  for each sample. By stepping down levels of the tree,  $J$  binary searches are computed in parallel to determine the containing bin of each random draw. At each level, the cached matrices tell the program whether to branch left or right by computing the branching threshold  $T$ , which is compared to the random draw  $r$ . The values in each column of  $X^{(p_j)}$  hold the current node index of each sample at level  $\ell$  of the search. At level  $L = \log_2 P$ , the algorithm continues the binary search locally on each processor until a row index is identified (a procedure we denote as “local-STS-CP”. For more details, see the original work [15]. At the end of the algorithm, the sample indices in  $X$  are correctly drawn according to

**Algorithm 4** STS-CP-build ( $U_i^{(p_j)}$ )

---

```

1:  $\tilde{G}_{\log_2 P} := U_i^{(p_j)\top} U_i^{(p_j)}$ 
2: for  $\ell = \log_2 P \dots 2$  do
3:   Send  $\tilde{G}_\ell$  to sibling of ancestor at level  $\ell$ , and receive the
   corresponding matrix  $\tilde{G}_{\text{sibling}}$ .
4:   Assign  $\tilde{G}_{\ell-1} = \tilde{G}_{\text{sibling}} + \tilde{G}_\ell$ 
5:   if Ancestor at level  $\ell$  is a left child then
6:      $\tilde{G}_{\ell-1}^L := \tilde{G}_\ell$ 
7:   else
8:      $\tilde{G}_{\ell-1}^L := \tilde{G}_{\text{sibling}}$ 
9:   Assign  $G_i := \tilde{G}_1$ 
10: Postcondition: Each processor stores a list of partial gram
    matrices  $\tilde{G}_\ell$  and  $G_i^L$ , from the root to its unique tree node.  $G_i$  is
    initialized.

```

---

**Algorithm 5** STS-CP-sample ( $k, J$ )

---

```

1: Initialize  $X \in \mathbb{Z}^{J \times N}, H \in \mathbb{R}^{J \times (R+1)}$  distributed by block rows.
   Let  $X^{(p_j)}, H^{(p_j)}$  be the block rows assigned to  $p_j$ .
2:  $X^{(p_j)} := [0], H^{(p_j)} := [1]$ 
3: for  $i = 1 \dots N, i \neq k$  do
4:    $G_{>k} := G^+ \otimes \bigotimes_{\ell=k+1}^N G_i$ 
5:    $H^{(p_j)}[:, R+1] := \text{uniform-samples}([0, 1])$ 
6:   for  $\ell = 1 \dots \log P - 1$  do
7:      $J^{\text{loc}} = \text{row-count} \left( X^{(p_j)} \right)$ 
8:     for  $k = 1 \dots J^{\text{loc}}$  do
9:        $r := H^{(p_j)} [k, R+1]$ 
10:       $h := H^{(p_j)} [k, 1 : R]$ 
11:       $X^{(p_j)} [i, k] * = 2$ 
12:       $T = h^\top \left( \tilde{G}_\ell^L \otimes G_{>k} \right) h / \left( h^\top \left( \tilde{G}_\ell \otimes G_{>k} \right) h \right)$ 
13:      if  $r \geq T$  then
14:         $X^{(p_j)} [i, k] += 1$ 
15:         $r := (r - T) / (1 - T)$ 
16:      else
17:         $r := r / T$ 
18:         $H^{(p_j)} [k, R+1] := r$ 
19:      Execute an All-to-allv call to redistribute  $X^{(p_j)}, H^{(p_j)}$ 
      according to the binary-tree data structure.
20:      $J^{\text{loc}} = \text{row-count} \left( X^{(p_j)} \right)$ 
21:     for  $k = 1 \dots J^{\text{loc}}$  do
22:        $\text{idx} := \text{local-STS-CP} \left( H^{(p_j)} [k, 1 : R], \tilde{G}_{\log_2 P}, G_{>k}, r \right)$ 
23:        $X^{(p_j)} [i, k] := \text{idx}$ 
24:        $H^{(p_j)} [k, 1 : R] * = U_i^{(p_j)} [\text{idx} - I_i p_j / P, :]$ 
25: return  $X^{(p_j)}, H^{(p_j)}$ 

```

---

the exact leverage scores of  $U_{\neq k}$ . The major communication cost of this algorithm stems from the **All-to-allv** collective between levels of the binary search. Because a processor may not have the required matrices  $\tilde{G}_\ell, \tilde{G}_\ell^L$  to compute the branching threshold for a sample, the sample must be routed to another processor that owns the information.

## REFERENCES

- [1] S. Smith, J. W. Choi, J. Li, R. Vuduc, J. Park, X. Liu, and G. Karypis, "FROSTT: The Formidable Repository of Open Sparse Tensors and Tools," 2017. [Online]. Available: <http://frostdt.io/>
- [2] H.-H. Mao, C.-J. Wu, E. E. Papalexakis, C. Faloutsos, K.-C. Lee, and T.-C. Kao, "MalSpot: Multi2 Malicious Network Behavior Patterns Analysis," in *Advances in Knowledge Discovery and Data Mining*, ser. Lecture Notes in Computer Science, V. S. Tseng, T. B. Ho, Z.-H. Zhou, A. L. P. Chen, and H.-Y. Kao, Eds. Cham: Springer International Publishing, 2014, pp. 1–14.
- [3] I. Balazevic, C. Allen, and T. Hospedales, "TuckER: Tensor Factorization for Knowledge Graph Completion," in *Proceedings of the 2019 Conference on Empirical Methods in Natural Language Processing and the 9th International Joint Conference on Natural Language Processing (EMNLP-IJCNLP)*. Hong Kong, China: Association for Computational Linguistics, Nov. 2019, pp. 5185–5194.
- [4] H. Kim and H. Park, "Sparse non-negative matrix factorizations via alternating non-negativity-constrained least squares for microarray data analysis," *Bioinformatics*, vol. 23, no. 12, pp. 1495–1502, 05 2007.
- [5] D. Hong, T. G. Kolda, and J. A. Duersch, "Generalized canonical polyadic tensor decomposition," *SIAM Review*, vol. 62, no. 1, pp. 133–163, 2020.
- [6] B. W. Larsen and T. G. Kolda, "Practical leverage-based sampling for low-rank tensor decomposition," *SIAM J. Matrix Analysis and Applications*, June 2022, accepted for publication.
- [7] S. Smith, K. Huang, N. D. Sidiropoulos, and G. Karypis, *Streaming Tensor Factorization for Infinite Data Sources*. SIAM, 2018, pp. 81–89.
- [8] T. G. Kolda and B. W. Bader, "Tensor Decompositions and Applications," *SIAM Review*, vol. 51, no. 3, pp. 455–500, Aug. 2009, publisher: Society for Industrial and Applied Mathematics.
- [9] J. H. Choi and S. Vishwanathan, "DFacTo: Distributed Factorization of Tensors," in *Advances in Neural Information Processing Systems*, Z. Ghahramani, M. Welling, C. Cortes, N. Lawrence, and K. Q. Weinberger, Eds., vol. 27. Curran Associates, Inc., 2014.
- [10] S. Smith, N. Ravindran, N. D. Sidiropoulos, and G. Karypis, "SPLATT: Efficient and Parallel Sparse Tensor-Matrix Multiplication," in *2015 IEEE International Parallel and Distributed Processing Symposium*, May 2015, pp. 61–70, iSSN: 1530-2075.
- [11] O. Kaya and B. Uçar, "Scalable sparse tensor decompositions in distributed memory systems," in *SC '15: Proceedings of the International Conference for High Performance Computing, Networking, Storage and Analysis*, 2015, pp. 1–11.
- [12] N. Park, B. Jeon, J. Lee, and U. Kang, "Bigtensor: Mining billion-scale tensor made easy," in *Proceedings of the 25th ACM International on Conference on Information and Knowledge Management*, ser. CIKM '16. New York, NY, USA: Association for Computing Machinery, 2016, p. 2457–2460.
- [13] D. Cheng, R. Peng, Y. Liu, and I. Perros, "SPALS: Fast Alternating Least Squares via Implicit Leverage Scores Sampling," in *Advances in Neural Information Processing Systems*, D. Lee, M. Sugiyama, U. Luxburg, I. Guyon, and R. Garnett, Eds., vol. 29. Curran Associates, Inc., 2016.
- [14] O. A. Malik, "More Efficient Sampling for Tensor Decomposition With Worst-Case Guarantees," in *Proceedings of the 39th International Conference on Machine Learning*. PMLR, Jun. 2022, pp. 14 887–14 917, iISSN: 2640-3498.
- [15] V. Bharadwaj, O. A. Malik, R. Murray, L. Grigori, A. Buluc, and J. Demmel, "Fast Exact Leverage Score Sampling from Khatri-Rao Products with Applications to Tensor Decomposition," in *Thirty-seventh Conference on Neural Information Processing Systems*, 2023. [Online]. Available: <https://arxiv.org/pdf/2301.12584.pdf>
- [16] S. Smith and G. Karypis, "A Medium-Grained Algorithm for Sparse Tensor Factorization," in *2016 IEEE International Parallel and Distributed Processing Symposium (IPDPS)*, May 2016, pp. 902–911, iISSN: 1530-2075.
- [17] M. W. Mahoney, "Randomized algorithms for matrices and data," *Foundations and Trends® in Machine Learning*, vol. 3, no. 2, pp. 123–224, 2011.
- [18] P. Drineas and M. W. Mahoney, "RandNLA: Randomized numerical linear algebra," *Commun. ACM*, vol. 59, no. 6, p. 80–90, may 2016.
- [19] P.-G. Martinsson and J. A. Tropp, "Randomized numerical linear algebra: Foundations and algorithms," *Acta Numerica*, vol. 29, p. 403–572, 2020.
- [20] I. Nisa, J. Li, A. Sukumaran-Rajam, P. S. Rawat, S. Krishnamoorthy, and P. Sadayappan, "An efficient mixed-mode representation of sparse tensors," in *Proceedings of the International Conference for High Performance Computing, Networking, Storage and Analysis*, ser. SC '19. New York, NY, USA: Association for Computing Machinery, 2019.
- [21] T. D. Ahle, M. Kapralov, J. B. T. Knudsen, R. Pagh, A. Velingker, D. P. Woodruff, and A. Zandieh, "Oblivious sketching of high-degree polynomial kernels," in *Proceedings of the Thirty-First Annual ACM-SIAM Symposium on Discrete Algorithms*, ser. SODA '20. USA: Society for Industrial and Applied Mathematics, 2020, p. 141–160.
- [22] C. Battaglino, G. Ballard, and T. G. Kolda, "A practical randomized cp tensor decomposition," *SIAM Journal on Matrix Analysis and Applications*, vol. 39, no. 2, pp. 876–901, 2018.
- [23] A. Gittens, K. Aggour, and B. Yener, "Adaptive sketching for fast and convergent canonical polyadic decomposition," in *Proceedings of the 37th International Conference on Machine Learning*, ser. Proceedings of Machine Learning Research, vol. 119. PMLR, 13–18 Jul 2020, pp. 3566–3575.
- [24] S. Smith and G. Karypis, "Tensor-matrix products with a compressed sparse tensor," in *Proceedings of the 5th Workshop on Irregular Applications: Architectures and Algorithms*, ser. IA<sup>3</sup>'15. New York, NY, USA: Association for Computing Machinery, 2015.
- [25] J. Li, Y. Ma, and R. Vuduc, "ParTII : A parallel tensor infrastructure for multicore cpus and gpus," Oct 2018, last updated: Jan 2020. [Online]. Available: <http://parti-project.org>
- [26] A. Nguyen, A. E. Helal, F. Checconi, J. Laukemann, J. J. Tithi, Y. Soh, T. Ranadive, F. Petriani, and J. W. Choi, "Efficient, out-of-memory sparse mttkrp on massively parallel architectures," in *Proceedings of the 36th ACM International Conference on Supercomputing*, ser. ICS '22. New York, NY, USA: Association for Computing Machinery, 2022.
- [27] E. T. Phipps and T. G. Kolda, "Software for sparse tensor decomposition on emerging computing architectures," *SIAM Journal on Scientific Computing*, vol. 41, no. 3, pp. C269–C290, 2019.
- [28] S. Wijeratne, R. Kannan, and V. Prasanna, "Dynasor: A dynamic memory layout for accelerating sparse mttkrp for tensor decomposition on multi-core cpu," 2023.
- [29] R. Kanakagiri and E. Solomonik, "Minimum cost loop nests for contraction of a sparse tensor with a tensor network," 2023.
- [30] G. Ballard, K. Hayashi, and K. Ramakrishnan, "Parallel nonnegative CP decomposition of dense tensors," in *2018 IEEE 25th International Conference on High Performance Computing (HiPC)*. IEEE, 2018, pp. 22–31.
- [31] U. Kang, E. Papalexakis, A. Harpale, and C. Faloutsos, "GigaTensor: scaling tensor analysis up by 100 times - algorithms and discoveries," in *Proceedings of the 18th ACM SIGKDD international conference on Knowledge discovery and data mining*, ser. KDD '12. New York, NY, USA: Association for Computing Machinery, Aug. 2012, pp. 316–324.
- [32] L. Ma and E. Solomonik, "Efficient parallel CP decomposition with pairwise perturbation and multi-sweep dimension tree," in *2021 IEEE International Parallel and Distributed Processing Symposium (IPDPS)*, May 2021, pp. 412–421, iISSN: 1530-2075.
- [33] E. Solomonik, D. Matthews, J. R. Hammond, J. F. Stanton, and J. Demmel, "A massively parallel tensor contraction framework for coupled-cluster computations," *Journal of Parallel and Distributed Computing*, vol. 74, no. 12, pp. 3176–3190, 2014, publisher: Academic Press.
- [34] R. Yadav, A. Aiken, and F. Kjolstad, "Spdistal: Compiling distributed sparse tensor computations," in *Proceedings of the International Conference on High Performance Computing, Networking, Storage and Analysis*, ser. SC '22. IEEE Press, 2022.
- [35] R. Jin, T. G. Kolda, and R. Ward, "Faster Johnson–Lindenstrauss transforms via Kronecker products," *Information and Inference: A Journal of the IMA*, vol. 10, no. 4, pp. 1533–1562, 10 2020.
- [36] H. Diao, Z. Song, W. Sun, and D. Woodruff, "Sketching for kronecker product regression and p-splines," in *International Conference on Artificial Intelligence and Statistics*. PMLR, 2018, pp. 1299–1308.
- [37] T. G. Kolda and D. Hong, "Stochastic Gradients for Large-Scale Tensor Decomposition," *SIAM Journal on Mathematics of Data Science*, vol. 2, no. 4, pp. 1066–1095, Jan. 2020.
- [38] E. Chan, M. Heimlich, A. Purkayastha, and R. van de Geijn, "Collective communication: theory, practice, and experience: Research Articles," *Concurrency and Computation: Practice & Experience*, vol. 19, no. 13, pp. 1749–1783, Sep. 2007.
- [39] T. B. Rolinger, T. A. Simon, and C. D. Krieger, "Performance considerations for scalable parallel tensor decomposition," *Journal of Parallel and Distributed Computing*, vol. 129, pp. 83–98, 2019.
- [40] H. M. Aktulga, A. Buluç, S. Williams, and C. Yang, "Optimizing sparse matrix-multiple vectors multiplication for nuclear configuration interaction calculations," in *2014 IEEE 28th International Parallel and Distributed Processing Symposium*, 2014, pp. 1213–1222.